J|A|C|S COMMUNICATIONS

Published on Web 01/28/2009

Initial Response of the Potassium Channel Voltage Sensor to a Transmembrane Potential

Werner Treptow,*,† Mounir Tarek,*,‡ and Michael L. Klein†

Center for Molecular Modeling and Department of Chemistry, University of Pennsylvania, Philadelphia, Pennsylvania, and UMR Structure et Réactivité des Systèmes Moléculaires Complexes, Nancy Université, CNRS, France

Received September 16, 2008; E-mail: mtarek@edam.uhp-nancy.fr; treptow@unb.br

In voltage-gated ion channels, the voltage-sensor (VS) domain senses the variations of the transmembrane (TM) voltage and triggers the conformational changes leading to the opening and closing of the pore.[1] During the voltage-sensing process, the displacement of the charges tethered to the VS gives rise to transient currents: the so-called gating currents. The time integral of this current is Q, the "gating charge" translocated across the membrane capacitance. Since the seminal work of Hodgkin and Huxley,[2] gating currents and gating charges have been measured for a variety of channels, as discussed extensively in recent reviews.[3,4] For channels selective for potassium (Kv), the total gating charge Q is ~13e (~3.25 per subunit).[5] Kinetic models devised to describe the time course of gating currents are very diverse, but all indicate that the gating process is complex, encompassing many *transitions* occurring at various characteristic time scales;[3,4,6−8] the fastest component resolved so far, the "loose" charge occurs within 10 μs.[9] Identification of the charges participating in gating currents has long served to signal potential conformational changes of the VS. Several basic residues in the S4 segment and negative charges in S2 and S3 have been implicated in voltage sensing.[10−14] Furthermore, salt bridges involving these charges appear to stabilize various gating *states* during activation.[15]

Accordingly, channel molecular models are testable against gating experiments to examine the robustness of the sensor geometry and gating motions.[16−18] Hence, given the known open state of the Kv1.2 channel and considering the total gating charge Q, models of the closed states of Kv channels[19,20] have been proposed.[21] However, determination of the closed-state topology does not allow full understanding of the gating mechanism. Key questions remain. What are the intermediate states? What is the pathway for charge gating? What elements of the structure can affect it? To begin to answer such questions, the dynamical, time-resolved gating processes need to be uncovered.

In this study, early *transition* events of the voltage sensor of the Kv1.2 potassium channel embedded in a lipid membrane are triggered using full atomistic molecular dynamics (MD) simulations spanning 50 ns. We follow the VS conformational changes when the system is subject to an applied hyperpolarized TM voltage and measure the corresponding gating charges. The results show that the channel reached a stable kinetic intermediate state, β', within 20 ns. The gating charge (~2e) associated with this fast *transition* resulted mainly from a *zipper-like* rearrangement of salt bridges involving negative charges in S2 and S3 and all but the two top residues R^{294} and R^{297} of S4. Interactions of the latter with phosphomoieties of the lipid head groups appear to stabilize the intermediate kinetic state β'. The gating charge measured here (~0.5e per subunit) is about the same magnitude as the elementary

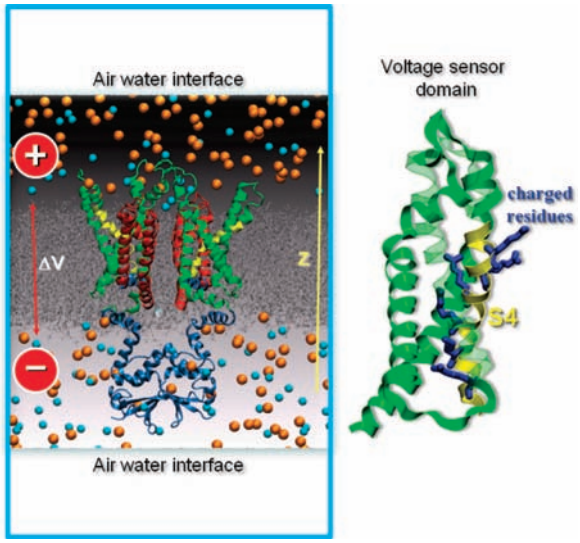

Figure 1. (Left) Initial MD configuration of Kv1.2 embedded in a POPC bilayer (gray) and ~150 mM KCl solution (VS: green, S4: yellow, pore: red, T1 intracellular tetramerization domain: blue, K^+: orange, Cl^-: cyan). For clarity, two of four channel subunits are depicted, and water is not shown. The MD simulation box is drawn in light blue. Note that the electrolytes extend up to the air/water interfaces. A net charge imbalance between the upper and lower electrolytes created by displacing cations from the lower to the upper bath induces a finite TM potential. (Right) One of the four voltage-sensor domains highlighting the charged residues (blue) of the S4 helix: from top to bottom: R^{294}, R^{297}, R^{300}, R^{303}, K^{306}, and R^{309}.

charge movements estimated from measurements of gating current fluctuations[7,22] and as the "loose" charges (~1e per subunit), indicating that the β' intermediate is of functional significance.

The Kv1.2 open (α) conformation has been thoroughly examined in previous simulations performed at depolarized potentials ($\Delta V = 0$ mV).[23] The VS domain (residues Pro^{156} to Ile^{316})) was shown to remain stable within a 10 ns time scale, in agreement with other simulations.[24] In contrast to an earlier investigation, in which an electric field was applied to generate ΔV,[25] here we used a method recently introduced.[26] In this setup, one considers a bilayer surrounded by electrolyte baths (150 mM KCl), each terminated by an air/water interface (Figure 1). As the bilayer behaves as a condenser, a finite transmembrane voltage ΔV may be imposed at $t = 0$ by creating a net charge imbalance q_0 between the intra- and extracellular electrolytes, i.e. displacing a given number of cations (depending on the system capacitance and total area) from the lower to the upper solution (cf. SM for details). As shown below, such a protocol allows for direct estimates of the gating charge Q.

Experimentally, the closed state is obtained within the millisecond time scale when ΔV is maintained at −100 mV.[1] Here, we applied ΔV about 6 times larger in order to promote a faster response of

† University of Pennsylvania.
‡ Nancy Université, CNRS.

10.1021/ja807330g CCC: $40.75

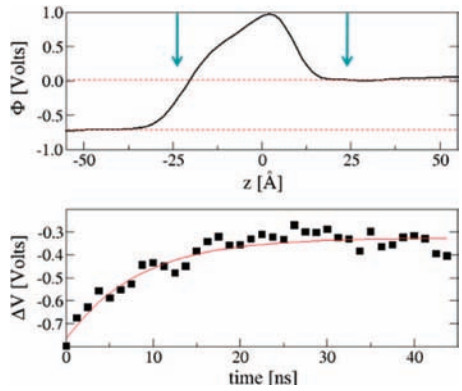

Figure 2. (Top) Electrostatic potential profile $\Phi(z)$ along the bilayer normal (z) of the initial configuration. $\Phi(z)$ is derived directly from the MD simulation as a double integral of the charge distribution of all atoms averaged over the membrane planes, $\rho(z)$, as $\Phi(z) - \Phi(0) = -\varepsilon_0^{-1}\int\int\rho(z'')dz''dz'$. Here, as a reference Φ is set to zero in the upper electrolyte. The arrows indicate the approximate position of the lipid/water interfaces. (Bottom) Relaxation of the TM potential during MD run. Every point corresponds to the TM voltage estimated from the average over a simulation-time window of ~1.2 ns; the error associated with each estimate is ±50 mV. The ΔV reduction provides a direct estimates of the gating charge (see main text).

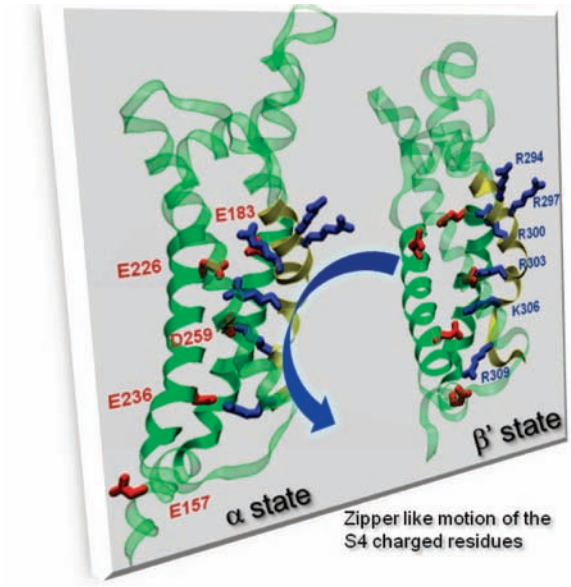

Figure 3. Initial (left) and final (right) conformations of a VS domain that are representative of respectively the α and β' states. The arrow highlights the collective motion of the lower charged residues of S4. Note the specific salt bridges between basic residues (blue) of S4 (yellow) and acidic residues (red) of segments S1, S2, and S3 (green).

the system (Figure 2). The channel was initially subject to a TM potential $\Delta V_{in} = -675$ mV. Given the size of the system, this necessitated displacing 4 K^+ ions ($q_0 = 8$) from the lower to the upper electrolytes (cf. SM). Within 20 ns, the TM potential relaxed to $\Delta V_{fin} \approx -325$ mV due to rearrangement of protein charges (Figure 3).

In the α conformation, the top residues R^{294} and R^{297} (S4) interact with lipid-PO_4^- groups at the membrane/water interface, and R^{300} is close to E^{183} (S1). Deeper within the VS, R^{303}, K^{306}, and R^{309} are involved respectively in salt bridges with E^{226} (S2), D^{259} (S3), and E^{236} (S2). During the $\alpha-\beta'$ transition, R^{300}, R^{303}, K^{306}, and R^{309} undergo a concerted downward motion relative to acidic residues. They moved from external to internal binding sites along the VS forming a different electrostatic network involving the pairs $R^{300}-E^{183}/E^{226}$, $R^{303}-D^{259}$, $K^{306}-E^{236}$ and $R^{309}-E^{157}$.

Table 1. Root Mean Square Deviations (rmsd) ([Å])

atoms	direction	VSD	S4	pore
heavy	*xyz*	6.2 ± 0.7	3.4 ± 0.6	2.4 ± 0.2
	z	3.2 ± 0.5	1.5 ± 0.3	1.0 ± 0.2
backbone	*xyz*	2.9 ± 0.3	1.4 ± 0.2	1.0 ± 0.1
	z	1.5 ± 0.3	0.6 ± 0.1	0.4 ± 0.1

The rmsd values are estimates of the overall displacement of selected protein segments between the initial and final conformations of the channel and are averaged over the four monomers.

The total rmsd between initial (α) and final (β') conformations of the VSD is 6.2 ± 0.7 Å. About 50% of this deviation is accounted-for by displacements along the membrane normal in which several S4 charged residues experienced side-chain rather than main-chain movements (Table 1). Note that the pore domain remained close to its initial state, e.g. open, and that most of the structural changes in the VS occurred during the first 20 ns (see Supporting Information).

As no free (K^+, Cl^-) ions translocated through the membrane during the MD run, the concomitant drop in ΔV (~350 mV) is mainly associated with rearrangement of tethered channel charges with respect to the membrane capacitor. In a closed circuit, e.g., a patch clamp experiment, maintaining ΔV constant requires balancing the capacitive current and leads therefore to a measure of gating currents. In this simulation protocol, as the capacitance of the system remains constant (see Supporting Information), the voltage drop provides a *direct* measure of a gating charge Q that is simply the measured change of ΔV. Evaluated as $Q = (q_0/2)\cdot(1 - (\Delta V_{fin}/\Delta V_{in}))$, it amounts here to ~2e.

For a structure undergoing a general $\alpha-\beta$ *transition* under ΔV, the gating charge Q may be linked[17,24] to the variation of the free energy of the channel through $Q\cdot\Delta V = \Delta G(\beta,\Delta V) - \Delta G(\alpha,\Delta V)$. In each conformational state λ, $\Delta G(\lambda,\Delta V) = G(\lambda,\Delta V) - G(\lambda,0) = \Delta V\cdot\Sigma q_i\cdot\delta_i^\lambda$ is the excess free energy due to the applied ΔV. Here, δ_i^λ is the so-called "electrical distance" that accounts for the degree of coupling between the local electrostatic potential $\phi_i^\lambda(r_i)$ and ΔV:[16,22,27,28] $\delta_i^\lambda \equiv \partial/\partial V(\phi_i^\lambda(r_i))$.

This formulation allows the identification of the specific molecular components that contribute to the gating charges (Figure 4). It shows that gating currents do not measure the displacement of charges across the membrane (i.e., across physical distances), but rather the product of the charges times the fraction of the membrane potential each traverses. Hence, as previously noted, while some S4 residues change their position from an intra to extracellular accessible space,[29,30] charge gating between *transition* states may involve limited displacements of the TM segments. The total gating charge per VS for the $\alpha-\beta'$ transition estimated from the MD trajectory (for details see Supporting Information) is $Q_{\alpha-\beta'} \approx -0.45$e and is very consistent with the *direct* measure (Figure 2). The electrical displacement during the *transition* $\delta^{\beta'} - \delta^\alpha$ is substantial for most of the VS charged residues and marginal in the loop regions. Importantly, several S2−S3 negatively charged residues—along with the S4 basic residues—contribute substantially to $Q_{\alpha-\beta'}$. These results are overall consistent with experiments[10−15] showing that mutations of the S2−S3 and S4 residues influence the gating currents and with recent simulations of the VS domain.[31]

In conclusion, the present MD study reveals the motions in the VS triggered by a TM voltage (ΔV) indicative of the existence of an early, fast *transition* state in which, S4 charged residues move relative to rather static acidic amino acids tethered to other VS segments. The Kv channel is formed by a tetramer in which the

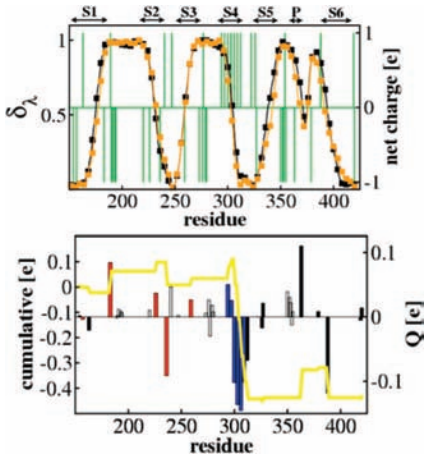

Figure 4. (Top) Electrical distances δ_i^λ for each TM residue in the α (black) and β' (orange) conformations and net charge per residue (green) along the Kv channel sequence (excluding the T1 domain). The position of the TM segments S1 to S6 and the P loop are indicated by arrows. δ_i^λ were normalized assuming $\delta_i^\lambda = 1$ and 0 for residues positioned respectively above 25 Å and below −25 Å from the bilayer center. (Bottom) Cumulative (yellow line) and per-residue (bars) gating charges. The S4-basic residues (blue) and the VS-negative residues (red: E157, E183, E226, E236, and D259) are highlighted. Contributions of the mobile loop residues (gray) were not included in the estimates of the cumulative charge.

voltage-sensors are decorrelated in the main structure (except through the tetramerization T1 intracellular domain). As such, the simulation results should in fact be viewed as four independent dynamical events in one single MD trajectory. Here, the $\alpha-\beta$ transition was observed in three of the four VS subunits (movies depicting the conformational change in each of the VS subunits are provided in the Supporting Information). This suggests that the transition described in the manuscript is not a rare event. The excess free-energy difference involved in the $\alpha-\beta'$ transition was directly estimated from the energetic formulation described above (equation[2] in the SM). For a ΔV value in the range of physiological TM potentials, i.e., 100 mV (3.86 kT/e), the stabilization of the β' state relative to the α state ($\Delta G(\beta',\Delta V) - \Delta G(\alpha,\Delta V)$ amounts to ∼1.5 kT. Note that this energy is related only to the transfer of protein charges across the TM electrical field, and it does not reflect the *overall* conformational free energy due to the $\alpha-\beta'$ transition.

Further analysis of the structure of the β' state indicates that the top S4 arginines R^{294} and R^{297} are in close contact with lipid-phosphate groups (cf. SM). The salt-bridge interactions involved are likely to play a key role in stabilizing the VS domain in its open state in agreement with recent experiments.[32] This may explain why the expected following transition, involving probably screw motions on the top of S4[33] in order to bring R^{294} and R^{297} from the membrane/water interface near the next binding site E^{183} (S1), requires longer time scales. Given suitable computational resources, a time-resolved atomistic description of such transitions, using the same protocols as in the present study, is within reach and should allow one to decipher further key steps and mechanisms underlying the exquisite sensitivity of Kv channels.

Acknowledgment. This research described herein was supported in part by the National Institutes of Health and the National Science Foundation through TeraGrid resources (NCSA).

Supporting Information Available: MD simulations protocols; details of the analyses methods; description of the conformational changes of the channel. This material is available free of charge via the Internet at http://pubs.acs.org.

References

(1) Hille, B. In *Ionic Channels of Excitable Membranes*, 2nd ed.; Sinauer: Sunderland, MA, 1992.
(2) Hodgkin, A. L.; Huxley, A. F. *J. Physiol.* **1952**, *117*, 500–544.
(3) Bezanilla, F. *Physiol. Rev.* **2000**, *80*, 555–592.
(4) Fedida, D.; Hesketh, J. C. *Prog. Biophys. Mol. Biol.* **2001**, *75*, 165–199.
(5) Schoppa, N. E.; McCormack, K.; Tanouye, M. A.; Sigworth, F. J. *Science* **1992**, *255*, 1712–1715.
(6) Zagotta, W. N.; Hoshi, T.; Aldrich, R. W. *J. Gen. Physiol.* **1994**, *103*, 3121–362.
(7) Schoppa, N. E.; Sigworth, F. J. *J. Gen. Physiol.* **1998**, *111*, 313–342.
(8) Loboda, A.; Armstrong, C. M. *Biophys. J.* **2001**, *81*, 905–916.
(9) Sigg, D.; Bezanilla, F.; Stefani, E. *Proc. Natl. Acad. Sci. U.S.A.* **2003**, *100*, 7611–7615.
(10) Papazian, D. M.; Timpe, L. C.; Jan, Y. N.; Jan, L. Y. *Nature* **1991**, *349*, 305–310.
(11) Perozo, E.; Santacruz-Toloza, L.; Stefani, E.; Bezanilla, F.; Papazian, D. M. *Biophys. J.* **1994**, *66*, 345–354.
(12) Aggarwal, S. K.; MacKinnon, R. *Neuron* **1996**, *16*, 1169–1177.
(13) Baker, O. S.; Larsson, H. P.; Mannuzzu, L. M.; Isacoff, E. Y. *Neuron* **1998**, *20*, 1283–1294.
(14) Tiwari-Woodruff, S. K.; Lin, M. A.; Schulteis, C. T.; Papazian, D. M. *J. Gen. Physiol.* **2000**, *115*, 123–138.
(15) Planells-Cases, R.; Ferrer-Montiel, A. V.; Patten, C. D.; Montal, M. *Proc. Nat. Acad. Sci. U.S.A.* **1995**, *92*, 9422–9426.
(16) Islas, L. D.; Sigworth, F. J. *J. Gen. Physiol.* **2001**, *117*, 69–89.
(17) Grabe, M.; Lecar, H.; Jan, Y. N.; Jan, L. Y. *Proc. Natl. Acad. Sci. U.S.A.* **2004**, *101*, 17640–17645.
(18) Chanda, B.; Asamoah, O. K.; Blunck, R.; Roux, B.; Bezanilla, F. *Nature* **2005**, *436*, 852–856.
(19) Pathak, M. M.; Yarov-Yarovoy, V.; Agarwal, G.; Roux, B.; Barth, P.; Kohout, S.; Tombola, F.; Isacoff, E. Y. *Neuron* **2007**, *56*, 124–140.
(20) Grabe, M.; Lai, H. C.; Jain, M.; Jan, Y. N.; Jan, L. Y. *Nature* **2007**, *445*, 550–553.
(21) Long, S. B.; Campbell, E. B.; MacKinnon, R. *Science* **2005**, *309*, 897–903.
(22) Sigworth, F. J. Q. *Rev. Biophys.* **1994**, *27*, 1–40.
(23) Treptow, W.; Tarek, M. *Biophys. J.* **2006**, *90*, L64–L66.
(24) Jogini, V.; Roux, B. *Biophys. J.* **2007**, *93*, 3070–3082.
(25) Treptow, W.; Maigret, B.; Chipot, C.; Tarek, M. *Biophys. J.* **2004**, *87*, 2365–2379.
(26) Delemotte, L.; Dehez, F.; Treptow, W.; Tarek, M. *J. Chem. Phys. B* **2008**, *112*, 5547–5550.
(27) Stevens, C. F. *Biophys. J.* **1978**, *22*, 295–306.
(28) Roux, B. *Biophys. J.* **1997**, *73*, 2980–2989.
(29) Mannuzzu, L. M.; Moronne, M. M.; Isacoff, E. Y. *Science* **1996**, *271*, 213–216.
(30) Cha, A.; Bezanilla, F. *Neuron* **1997**, *19*, 1127–1140.
(31) Nishizawa, M.; Nishizawa, K. *Biophys. J.* **2008**, *95*, 1729–1744.
(32) Schmidt, D.; Jiang, Q.-X.; MacKinnon, R. *Nature* **2006**, *444*, 775–779.
(33) Campos, F. V.; Chanda, B.; Roux, B.; Bezanilla, F. *Proc. Natl. Acad. Sci. U.S.A.* **2007**, *104*, 7904–7909.

JA807330G